Brain Oscillatory Activity during Spatial Navigation: Theta and Gamma Activity Link Medial Temporal and Parietal Regions

David J. White[1], Marco Congedo[2], Joseph Ciorciari[1], and Richard B. Silberstein[1]

Abstract

■ Brain oscillatory correlates of spatial navigation were investigated using blind source separation (BSS) and standardized low resolution electromagnetic tomography (sLORETA) analyses of 62-channel EEG recordings. Twenty-five participants were instructed to navigate to distinct landmark buildings in a previously learned virtual reality town environment. Data from periods of navigation between landmarks were subject to BSS analyses to obtain source components. Two of these cortical sources were found to exhibit significant spectral power differences during navigation with respect to a resting eyes open condition and were subject to source localization using sLORETA. These two sources were localized as a right parietal component with gamma activation and a right medial-temporal–parietal component with activation in theta and gamma bandwidths. The parietal gamma activity was thought to reflect visuospatial processing associated with the task. The medial-temporal–parietal activity was thought to be more specific to the navigational processing, representing the integration of ego- and allo-centric representations of space required for successful navigation, suggesting theta and gamma oscillations may have a role in integrating information from parietal and medial-temporal regions. Theta activity on this medial-temporal–parietal source was positively correlated with more efficient navigation performance. Results are discussed in light of the depth and proposed closed field structure of the hippocampus and potential implications for scalp EEG data. The findings of the present study suggest that appropriate BSS methods are ideally suited to minimizing the effects of volume conduction in noninvasive recordings, allowing more accurate exploration of deep brain processes. ■

INTRODUCTION

Medial-temporal lobe structures, the hippocampus in particular, have been implicated in the process of spatial navigation. After identifying "place cells" in the rodent hippocampus, which fired on the basis of position in the environment, O'Keefe and Nadel (1978) postulated a cognitive map of the environment stored within the hippocampus. Single-unit recordings have since demonstrated the presence of hippocampal cells with similar properties in primates (Hori et al., 2005; Matsumura et al., 1999) and humans (Ekstrom et al., 2003). Hippocampal place cells interact with cells from surrounding structures, including grid cells of the entorhinal cortex (Hafting, Fyhn, Molden, Moser, & Moser, 2005) to provide a representation of space (Moser, Kropff, & Moser, 2008). Functional neuroimaging has enabled exploration of brain processes involved in human spatial navigation, using virtual reality (VR) tasks to simulate navigation through realistic 3-D environments. This research has consistently shown increased activity in the right medial-temporal lobe as well as parietal regions, among a network of active areas during navigation (Iaria, Chen, Guariglia, Ptito, & Petrides, 2007; Hartley, Maguire, Spiers, & Burgess, 2003; Grön, Wunderlich, Spitzer, Tomczak, & Riepe, 2000; Maguire et al., 1998). Furthermore, neuropsychological testing of humans with damage to the hippocampus and surrounding medial-temporal lobe has demonstrated a number of spatial processing and memory deficits (Lee et al., 2005; Parslow et al., 2005; Astur, Taylor, Mamelak, Philpott, & Sutherland, 2002; Nunn, Graydon, Polkey, & Morris, 1999; Bohbot et al., 1998).

Recent models of spatial processing have integrated findings from rodent research, functional neuroimaging, and neuropsychological deficits in humans, working to highlight a role for medial-temporal lobe and parietal regions. The hippocampus and surrounding medial-temporal lobe structures are thought to be important for long-term allocentric (world-centered) representations of the environment, whereas the parietal lobe has been proposed as providing short-term egocentric (self-centered) representations within the environment (Burgess, 2008; Whitlock, Sutherland, Witter, Moser, & Moser, 2008; Byrne, Becker, & Burgess, 2007). In reviewing recent progress in the understanding of the medial-temporal lobe in spatial processing, Moser et al. (2008) highlight the gap in understanding

[1]Swinburne University of Technology, [2]Grenoble University

as to how spatial representations of the medial-temporal lobe interact with other regions, such as the parietal lobe, also important for spatial navigation. In line with rodent findings, Byrne et al. (2007) propose the theta rhythm is ideally suited to facilitate communication between medial-temporal lobe and parietal regions. However the importance of gamma and theta oscillations in long-term representations of space in the rodent hippocampus has been demonstrated (for a review, see Lisman, 2005). Furthermore, recordings from rodent hippocampus and neocortex suggest neocortical gamma phase is modulated by hippocampal theta (Sirota et al., 2008), and theta–gamma coupling has been proposed as a neural coding system beyond the hippocampus (Lisman & Buzsáki, 2008; Lisman, 2005). From this, one may speculate that theta and gamma activity facilitate the information transfer of different spatial representations required for successful navigation.

Much of the research exploring oscillatory correlates of human spatial navigation has utilized intracranial EEG (iEEG) recordings because of the difficulties in recording activity from the implicated deep medial-temporal regions. Using iEEG recordings from epileptic patients during VR maze navigation, task-dependent theta bursts have been identified in subdural grid electrodes in neocortex (Caplan, Madsen, Raghavachari, & Kahana, 2001; Kahana, Sekuler, Caplan, Kirschen, & Madsen, 1999). Expanding on these findings, Caplan et al. (2003) found navigation-related theta activity across cortical sites during VR town navigation, which was later shown to covary with navigation-related hippocampal theta (Ekstrom et al., 2005). Although supporting the hypothesized role for theta integrating allocentric information from the hippocampus with other cortical regions required for successful navigation, work from this research group has also highlighted navigation-related activity in numerous frequency ranges, including gamma oscillations (Jacobs et al., 2010; Ekstrom et al., 2005; Caplan et al., 2001).

Noninvasive techniques such as EEG and magnetoencephalography (MEG) provide an opportunity to explore this relationship in larger samples of healthy volunteers. EEG studies of maze navigation have reported increased theta power (Bischof & Boulanger, 2003) and increased theta coherence between right parietal and temporal regions (Mackay, Kirk, Hamm, & Johnson, 2001). However, such analyses do not facilitate any real conclusions as to the involvement of the medial-temporal lobe in spatial navigation. Complicating matters further, the hippocampus has traditionally been viewed as a closed field structure (e.g., Fernández et al., 1999)—isopotentially zero external to the hippocampus proper because of its cellular architecture (Lorente de Nò, 1947)—making any inferences as to hippocampal activity from noninvasive recordings difficult. Although some reports have challenged the notion of the hippocampus as a closed field structure, anatomically and electrophysiologically realistic modeling of the hippocampus and other deep structures suggests noninvasive EEG and MEG may in fact be capable of localizing such activity (Attal et al., 2009) and hippocampal theta has been reported using MEG (Tesche & Karhu, 2000); direct evidence is lacking, which would allow firm conclusions as to hippocampal contribution to surface-recorded EEG. Regardless, it has been proposed that task-induced scalp theta activity may provide an indirect "window" with which to view cortico-hippocampal communication (Bastiaansen & Hagoort, 2003).

Elevated theta power associated with VR navigation has been demonstrated using MEG (Cornwell, Johnson, Holroyd, Carver, & Grillon, 2008; de Araújo, Baffa, & Wakai, 2002). Using a VR town navigation task, a strong increase in theta power during periods of navigation was localized to temporal and parietal regions using a single current dipole model; the authors concluded that more sophisticated source modeling could provide more definitive evidence of medial-temporal involvement (de Araújo et al., 2002). Using a beam-former spatial filtering technique, elevated theta activity during navigation using a modified VR Morris water maze was observed in the left hippocampal and parahippocampal regions (Cornwell et al., 2008). This left medial-temporal lobe activity was found to correlate with successful navigation. Subsequent exploratory analysis of the whole-brain volume revealed theta sources were largely confined to the left temporal and frontal regions. The use of an "aimless movement" control condition may have understated the role of other important parts of the navigation network, given previous reports of virtual movement suggest the presence of "movement-related theta" (Ekstrom et al., 2005). If a significant portion of the network is active during any virtual movement, the use of such a condition for contrast may explain why theta source activity was only observed in left medial-temporal regions, in contrast with much of the navigation literature showing either bilateral or right-lateralized involvement.

Given that the magnetic field of a deep dipolar source will fall off at a rate greater than the equivalent electric field (Nunez & Srinivasan, 2006), EEG may represent a more natural candidate for the study of deep regions, such as the medial-temporal lobe. Still, deep sources represent a challenging scenario for EEG source localization techniques; as observed, EEG is the sum of activity from widespread brain sources (plus artifacts) as a result of volume conduction (Nunez & Srinivasan, 2006), and superficial or strong sources make deeper or weaker sources difficult to localize with popular source localization techniques such as standardized low resolution electromagnetic tomography (sLORETA; see, e.g., Wagner, Fuchs, & Kastner, 2004). Recently, data-independent and data-driven spatial filters have been applied to EEG data as a means of minimizing the effects of volume conduction, thus enhancing the sensitivity of source localization techniques (Congedo, 2006; Onton, Westerfield, Townsend, & Makeig, 2006).

Blind source separation (BSS) is a group of processing techniques that seek to identify source activity from a mixed signal and has been employed in a variety of fields,

including speech processing (Jang, Lee, & Oh, 2002), face recognition (Yuen & Lai, 2002), wireless communication (van der Veen, Talwar, & Paulraj, 1997), and radar applications (Fiori, 2003), and with a range of biomedical signals (James & Hesse, 2005). In EEG data, BSS has been used for the identification and removal of artifacts (Romero, Mañanas, & Barbanoj, 2008; Delorme, Sejnowski, & Makeig, 2007) and to provide source identification before a source localization step (Mutihac & Mutihac, 2007). After decomposing the observed EEG into a number of elementary additive sources, subsequent source localization is more reliable, typically capable of exact localization of single equivalent dipoles. BSS techniques have been used to enhance source localization efforts with ERP data (Grau, Fuentemilla, & Marco-Pallarés, 2007; Marco-Pallarés, Grau, & Ruffini, 2005), ictal EEG in epilepsy (Leal et al., 2007, 2008), and task-related time–frequency domain EEG (Huang, Jung, Delorme, & Makeig, 2008; Delorme, Westerfield, & Makeig, 2007; Onton, Delorme, & Makeig, 2005).

Several BSS methods, including independent component analysis, exist. On the basis of physiological and statistical consideration, the approximate joint diagonalization of Fourier cospectral matrices (AJDC) has been suggested as a method well suited to EEG data (Congedo, Gouy-Pailler, & Jutten, 2008). In its basic form, AJDC seeks a linear transformation of the data jointly diagonalizing Fourier cospectral matrices at multiple frequencies. As these matrices hold in the off-diagonal part the in-phase covariance of all pairwise EEG sensors, their diagonalization produces spatial filters extracting uncorrelated sources. Because the diagonalization set includes several frequencies, one is assured to extract source components as long as they have nonproportional power spectra, whereas each isolated component may involve either focal or distributed regions oscillating synchronously (in-phase with same or opposite sign) at the same frequencies. Using this AJDC approach, components obtained from scalp EEG recordings have demonstrated high correlations with simultaneously recorded subdural iEEG in a study on tinnitus (van der Loo, Congedo, Plazier, Van de Heyning, & De Ridder, 2007). More recently, the AJDC method has been extended to group data analysis to obtain a common set of filters describing the sample under study (Congedo, John, De Ridder, & Prichep, 2010).

The aim of the present work was to pursue this line of inquiry, exploring the generators of brain oscillatory activity in spatial navigation, using group BSS to identify sources that could then be subject to source localization methods. On the basis of recent models of spatial cognition and research using iEEG and MEG, it was hypothesized that navigation would be associated with increased medial-temporal lobe and parietal lobe activity, particularly in the theta frequency band. The novelty of the present study in the context of the existing literature on spatial navigation resides in the use of a group BSS method applied to scalp EEG to visualize medial-temporal lobe activity.

METHODS

Participants

The sample consisted of 25 healthy, right-handed volunteers with normal or corrected-to-normal vision and no history of head injury, epilepsy, or psychiatric diagnoses (13 women, $M = 24.62$, $SD = 4.84$; 12 men, $M = 24.75$, $SD = 4.83$). All participants reported experience with computer and video games, the majority rating themselves as "occasional users." Written informed consent was obtained from all participants, in accordance with the Swinburne University Research Ethics Committee.

EEG Acquisition

EEG activity was recorded using an electrode cap with 62 scalp electrodes positioned according to the extended 10–10 system (Quik-Caps; Neuroscan, Inc., Abbotsford, Victoria, Australia). On-line recordings were referenced to an electrode positioned between Cz and Cpz, with a ground electrode between Fz and Fpz. To monitor eye movement and blinks, additional electrodes were placed on the infraorbital and supraorbital regions of the left eye as well as a bipolar channel located at the outer canthi of each eye. Recordings were also taken from both left and right mastoids to facilitate a linked mastoid reference in off-line analysis. Electrode impedance at all sites was maintained below 5 kΩ. EEG recordings were digitized at 500 Hz with a band-pass filter between 0.1 and 70 Hz and a notch filter at 50 Hz (single-pole Butterworth, 6 dB down at cutoffs) using the SynAmps2 amplifier system and Scan 4.3 Acquisition software (Neuroscan, Inc.).

Procedure

Participants were seated 60 cm from a 17-in. LCD monitor in a dimly lit room. Baseline eyes open (2.5 min, fixation on center of blank screen) and eyes closed (2.5 mins) recordings were obtained, followed by completion of an EOG calibration task comprising a series of blinks and left, right, up, and down eye movements (calibration data was not utilized for this study). At this time, participants were given 10 min to learn the layout of the VR town where no active instructions or buttons were present within the town (see town description below). Participants were instructed to try and form a mental representation of the layout of the town, paying particular attention to the landmark buildings. Pilot testing indicated 10 min was sufficient time to successfully learn the layout of the town (pilot participants were allowed to navigate through the town for as long as desired, until they felt they knew the location of all landmarks, after which time they were given a generic topographic map with the same street and building layout as the town, only with blank buildings. Participants were required to indicate where each of the landmarks was located; 10 min ensured correct identification of landmark locations). After the learning period, an unrelated

simplified navigation task was carried out where subjects were required to move themselves within a small virtual room so as to face a particular orientation with respect to a central landmark (used in Seixas, Brotchie, Crewther, & Ip, 2006). The primary purpose of this period was to provide a delay of at least 5-7 mins between learning the town layout and beginning the navigation task. Recordings were then made while participants completed the navigation task.

Virtual Town Navigation

Using the high-resolution adaptation of Duke Nukem 3D (Duke Nukem 3D: 3D Realms Entertainment, Apogee Software Ltd. Garland, TX; High-Resolution Pack: GNU General Public License), the VR town was created using the associated map editor software (BUILD, Ken Silverman, 3D Realms Entertainment). Resolution of the enhanced version is 1280 × 1024; four times the resolution of the original. As with recent town navigation studies, a simple town was deemed appropriate to facilitate completion of the task in similar times across participants and ensure comparison of accurate navigation only (de Araújo et al., 2002). The town consisted of a 5 × 4 grid of streets and a series of buildings, including six city landmarks: a cinema, an aquarium, a restaurant, a fire station, a pyramid, and a bar (Figure 1A). Participants navigated from a 3-D first-person (see Figure 1B) view using the four arrow keys on a standard computer keyboard and used the space bar to press a button located at each landmark. At the beginning of the navigation condition, participants were required to push a button at their start location, at which time instructions appeared to navigate to one of the landmark buildings. Upon arrival at that landmark, they were again required to find and push a button located on the landmark, then follow further instructions to navigate to another landmark building. Participants navigated to each of the six landmark buildings once, pushing a button located on the target building, which provided instructions to move onto another landmark. Navigation task completion was recorded and reviewed to quantify performance.

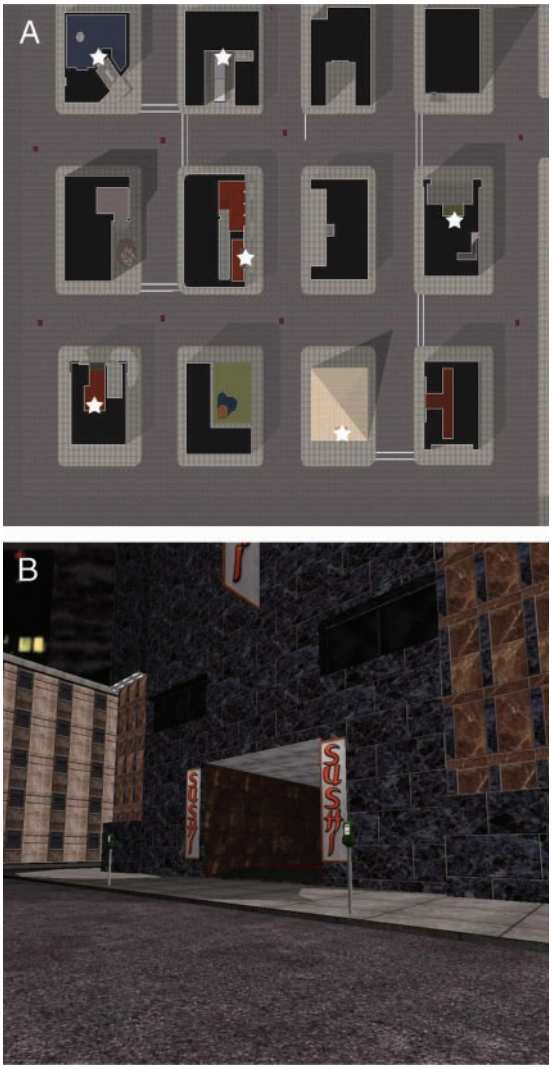

Figure 1. Navigation task. (A) Layout of the town with stars indicating location of landmarks. (B) First-person view from within the town.

EEG Data Preprocessing

Baseline and navigation recordings were rereferenced to a linked mastoid reference and band-pass filtered (FIR, 24 dB/octave) in the range of 1–44 Hz using Scan 4.3 Edit Software (Neuroscan, Inc.). The first 8 sec of navigation to each of the six landmarks were selected for each participant. Eight seconds corresponded to the minimum time for a participant to travel the distance between the closest two landmarks, ensuring the participant was actively navigating throughout the selected period. This resulted in 48 sec of navigation data for each participant (6 landmarks × 8 sec). Baseline eyes open data of the same length was selected from approximately 20 sec into the resting eyes open recording. To facilitate further computation, all data were down-sampled to 128 Hz using a natural cubic spline interpolation routine (Congedo, Ozen, & Sherlin, 2002). Both segments of navigation and baseline data, including the 62 EEG electrodes and the two vertical EOG channels, were concatenated into a single file for each participant.

For each participant, data were then decomposed using AJDC (Congedo et al., 2008), whereupon the most energetic EOG component and EMG component were identified and removed from the data by linear filtering using the ICoN software.[1] The AJDC algorithm consisted of estimating 1-Hz resolution Fourier cospectral matrices (Bloomfield, 2000, p. 207) by fast Fourier transform, averaging over 50% overlapping 1-sec epochs as per the well-established Welch method (Welch, 1967). A Welch tapering window was multiplied to each epoch to reduce side-lobe effects in fast Fourier transform estimations. Then, the approximate joint diagonalization for average cospectra

in the range of 1–28 Hz was obtained using the algorithm proposed by Tichavský and Yeredor (2009). Following our previous studies, this upper limit for the diagonalization set (28 Hz) followed the analysis of grand-average cospectral structures. For frequencies above 28 Hz, it was verified in our data that the cospectral matrices become more and more diagonal, indicating a dropping of the signal-to-noise ratio. Thus, limiting the approximate joint diagonalization to lower frequency effectively allows a more noise-resistant estimation of the spatial filters. Nonetheless, such spatial filters apply equally well to all frequencies because of the assumption of a linear instantaneous mixing model (Congedo et al., 2008, 2010).

Group Analysis

Group BSS analysis followed four steps: (a) source identification using BSS, (b) testing for sources demonstrating spectral power differences from baseline to navigation, (c) source localization of those source components demonstrating spectral power changes, (d) correlating spectral power with navigation performance for those sources and bands showing significant task-related activity. The group AJDC algorithm diagonalizes the grand average of cospectral matrices. Because we are interested in brain activity related to spatial navigation, the grand average ($n = 25$) was computed on navigation data only. The AJDC algorithm specifications were as previously, but in this case, a subspace reduction by truncated whitening limited the estimated components to 36, allowing more than 99% of explained variance to be preserved in the solution (mean square representation error = 0.0093). Such a subspace reduction strategy improves the signal-to-noise ratio while preserving the data of interest and makes the ensuing analysis more easily interpretable.

For each of the group source components obtained from the navigation condition, log-transformed spectral power in the range of 1–44 Hz was computed in 1-Hz frequency bins for both navigation and baseline condition for each subject separately. Finally, a rank-transformed permutation *t* max test (Westfall & Young, 1993) was used to determine frequency bands where navigation and baseline source power significantly differed (30,000 random permutations). This method automatically corrects for the number of simultaneously tested null hypotheses (multiple comparisons) along frequencies within each component, whereas a Bonferroni-adjusted significance threshold of $p = .00139$ was used to control for multiple comparisons across the 36 components (0.05/36). Source components displaying significant results were localized in cortical space by applying the sLORETA inverse solution, after centering (referencing to the common average, which is necessary for sLORETA estimations; Congedo et al., 2008) the corresponding column of the estimated BSS mixing matrix. For the sLORETA inverse solution (Pascual-Marqui, 2002), the regularization parameter (Tikhonov regularization; see Congedo, 2006) was set to 10^3. We used the head model of the Key Institute for Brain–Mind Research (Zurich, Switzerland), which incorporates a three-shell spherical head model coregistered to the anatomical brain atlas of Talairach and Tournoux (1988) and makes use of standard EEG electrode coordinates derived from cross-registration between spherical and realistic head geometry (Towle et al., 1993). The solution space is restricted to cortical gray matter using the digitized probability atlas of the Brain Imaging Center at the Montreal Neurological Institute (Collins, Neelin, Peters, & Evans, 1994), divided in 2394 voxels, measuring $7 \times 7 \times 7$ mm.

Spectral power estimates for scalp electrode sites were obtained from the same navigation and resting eyes open data sets used in the group BSS analysis. These spectral estimates followed the same procedure as that used to derive spectral estimates used as part of the group BSS analysis. The same rank-transformed permutation *t* max test (Westfall & Young, 1993) was used to determine frequency bands where navigation and baseline scalp electrode spectral power significantly differed. This analysis used the same significance testing strategy as for the group BSS sources, where the *t* max test controls for multiple comparisons across frequencies and Bonferroni correction was used to control for the comparisons across all electrodes (0.05/62 = 0.0008). Scalp maps of *t* scores contrasting grand average power spectra during navigation versus eyes open baseline condition were also generated to explore those electrode locations where power in the theta band increased beyond baseline levels.

RESULTS

Task performance was quantified as the summed latency (in seconds) from initiation of each block of navigation to arrival at each landmark. Although the task was designed to be relatively easy, variable performance was apparent across participants (mean latency = 151.64 sec, *SD* = 11.67). As walking speed within the task was uniform, greater latency reflects greater distance travelled to reach landmarks and, thus, less efficient navigation. This performance could then be correlated with those measures of brain activity that show modulation by the task.

Group BSS Results

Three source components showed frequency bandwidths that significantly differed from baseline to navigation at the strict level of significance:[2] Components 2, 5, and 6 (Table 1). Component 6 was deemed to be an artifactual component; thus, it will be discussed separately.

Component 2 was localized to right parieto-occipital regions, showing greater beta and gamma power during navigation. Although the significant voxels comprised an extended area, the sLORETA solution shows a focal right parietal distribution centered in inferior parietal gyrus. Component 5 was largely localized to right parietal and

Table 1. Overview of Source Components with Significant Differences from Baseline to Navigation

		Most Significant Voxels			
		Talairach Coords			
	Frequency Bandwidths (Navigation > Control)	*x*	*y*	*z*	*Region*
Component 2	28 Hz; 42–44 Hz**	60	−39	29	inferior parietal (R)
		−59	−60	36	supramarginal gyrus (L)
		32	−88	29	superior occipital (R)
		−59	−4	29	precentral gyrus (L)
		−31	−88	36	precuneus (L)
Component 5	3–4 Hz**	4	−60	50	precuneus (R)
		32	−53	50	superior parietal (R)
	3–6 Hz; 44 Hz*	32	−25	15	insula (R)
		4	−11	−6	parahippocampal gyrus (R)
		18	−11	−13	parahippocampal gyrus (R)
Component 6	1–6 Hz**	−38	17	−13	inferior frontal (L)
		39	45	1	inferior frontal (R)
		25	52	1	superior frontal (R)
		−24	45	15	medial frontal (L)
		−24	52	1	superior frontal (L)

*p = .0056.

**p = .00139.

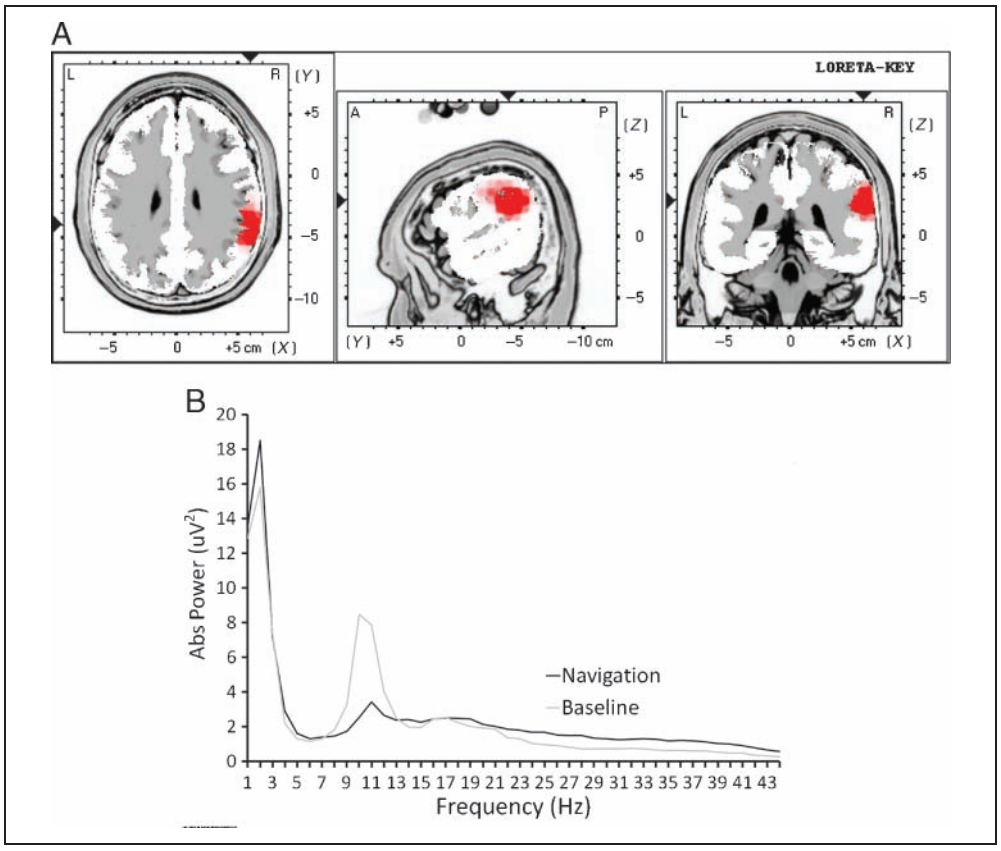

Figure 2. (A) sLORETA source map of Component 2, from left to right: axial, sagittal, and coronal sections. A = anterior, P = posterior, L = left, R = right. (B) Power spectra for Component 2 during navigation and baseline conditions.

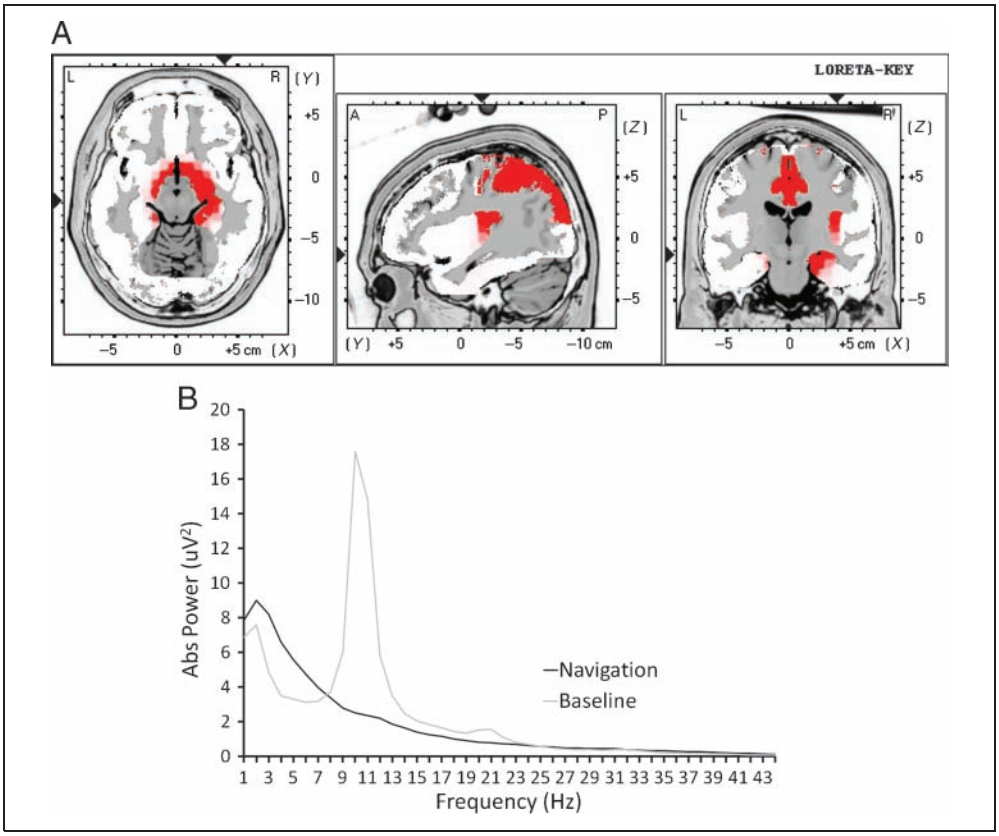

Figure 3. (A) sLORETA source maps for Component 5, from left to right: axial, sagittal, and coronal sections. A = posterior, P = posterior, L = left, R = right. (B) Power spectra for Component 5 during navigation and baseline conditions.

medial-temporal lobe regions, with significantly elevated theta power during navigation. As with de Araújo et al. (2002), peak theta activity was at the low end of the traditionally defined bandwidth. Unlike Component 2, the sLORETA solution demonstrated multiple sources, with both right parietal and medial-temporal regions implicated. Using a less stringent significance threshold (0.2/36; $p = .0056$), the active theta bandwidth was larger, and a marginally significant increase in gamma power was also noted on this component during navigation.[3] The source localization and power spectra of the two cortical sources found to show navigation-related activity are presented in Figures 2 and 3.

Component 6 demonstrated a bilateral frontal scalp distribution (F7 and F8 centered), was localized to inferior frontal regions, and showed significantly greater power in the 1–6 Hz bandwidth during navigation. This was deemed eye movement artifact, induced by exploring the visual environment presented within the task. Although the most energetic eye artifact component was removed during preprocessing, the removed artifact was likely eye blinks, and Component 6 represents remaining lateral eye movement.

Finally, bands showing spectral power increases during navigation for Components 2 and 5 were correlated with navigation latency. Continuous bins to show significant increases were pooled, resulting in power estimates for four separate bands (Component 2: gamma [42–44 Hz] and beta [28 Hz]; Component 5: theta [3–6 Hz] and gamma [44 Hz]), which were then log transformed. Spectral data for each band was then plotted against navigation latency and inspected for outliers, and Spearman rank correlations were calculated. Two outliers were removed from the correlation analyses. A significant negative association between Component 5 theta and navigation latency was observed ($r_s = -.659$, $p = .001$). Greater theta power on this medial-temporal–parietal source was associated with more efficient navigation (see Figure 4).

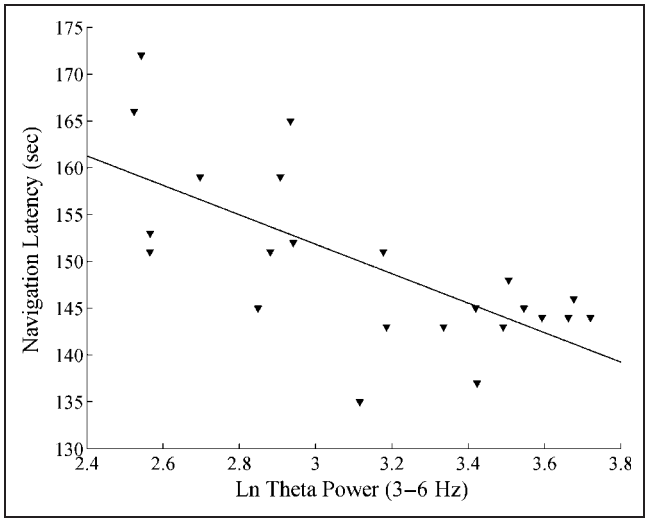

Figure 4. Scatterplot of navigation latency against Component 5 theta (3–6 Hz) power during navigation.

No association was observed between spectral data for Component 2 gamma and beta or Component 5 gamma and performance.

Scalp EEG Analysis

Average spectral power at scalp electrode sites was obtained for both baseline and navigation conditions. Representative power spectra at a number of scalp sites are presented for the navigation condition (Figure 5A). Results of the permutation *t* max tests showed that only increased power at 1 and 2 Hz was observed at electrodes F7, F4, and F6. This is presumably the result of such a strict significance threshold and the lower signal-to-noise ratio of scalp analyses. To further probe scalp sites showing theta power differences during navigation, scalp maps of *t* scores obtained from contrasting spectral power during navigation with that of baseline spectral power were obtained. Scalp maps of these *t* scores in the lower theta band are shown in Figure 5B. Sites where theta power increased from baseline to navigation were largely confined to parieto-occipital regions. The increased theta in lateral frontal sites is likely the same EOG artifact isolated in Component 6 of the BSS solution. Thus, although theta power was maximal around the frontal midline, theta power in this region did not increase from the resting eyes open condition, rather it was theta power in more posterior regions that increased during navigation.

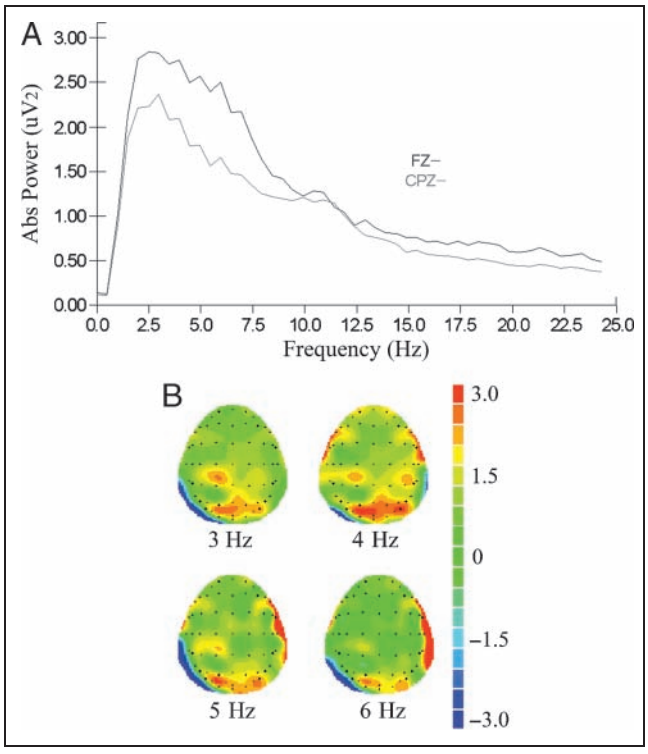

Figure 5. (A) Representative grand average power spectra for scalp electrode sites Fz and CPz during navigation. (B) Scalp maps of *t* scores for average spectral power from 3 to 6 Hz during navigation contrasted with baseline spectral power. Positive *t* scores indicate greater power in navigation condition.

DISCUSSION

The present study utilized BSS and source localization of high-density EEG recordings to further explore brain correlates of spatial navigation. In line with predictions, two source components showed significant navigation-related activity: a right parietal source with elevated beta and gamma activity and a right medial-temporal–parietal source with increased theta and gamma activity. Theta activity from this source was correlated with navigation performance, where greater theta activity was associated with more efficient navigation. These findings are in agreement with the bulk of the literature exploring navigational processing, further supporting recent models of spatial cognition in highlighting the role of parietal and medial-temporal lobe regions (Burgess, 2008; Whitlock et al., 2008; Byrne et al., 2007). That such results were obtained using scalp-recorded EEG suggests noninvasive techniques, such as this may offer legitimate tools for the investigation of complex cognitive processes involving generators beyond those immediately proximal to the surface.

Gamma Activity in the Right Parietal Region

The right inferior parietal source with activation in beta and gamma bands likely reflects visuospatial processing induced by the task. Right-lateralized gamma activity has also been reported in a recent iEEG study using virtual town navigation associated with movement- and search-related processing, particularly in temporal, parietal, and occipital electrode placements (Jacobs et al., 2010). Given the role of the parietal lobe in numerous aspects of spatial cognition, including basic visuospatial processing and egocentric representations of space, gamma activity in this region likely reflects the importance of these processes during spatial navigation.

Theta or Gamma Activity in Right Medial-temporal–Parietal Regions

Given that the BSS method we employed (AJDC) specifically seeks uncorrelated components with nonproportional power spectra, multiple regions identified on a single component can be conceived as a network oscillating in-phase (with same or opposite sign) at the same frequency. Thus, in the present research, a medial-temporal–parietal network emerged during spatial navigation displaying in-phase theta activity as well as in-phase gamma activity. Although the medial-temporal lobe has long been implicated in allocentric representations of the environment and the precuneus of the parietal lobe thought to be important for egocentric representations of environment, our findings suggest a coupling between the two regions during

navigation. Such coupling will form the object of a dedicated investigation.

Although the use of a resting eyes-open contrast condition does not control for nonspecific factors, the observation that this theta activity is correlated with navigation performance links this activity with efficient navigation. Gamma and theta oscillations have been linked with numerous aspects of human spatial navigation using iEEG (Jacobs et al., 2010; Ekstrom et al., 2005; Caplan et al., 2001) and MEG (Cornwell et al., 2008, 2010; de Araújo et al., 2002). Our findings replicate observed theta and gamma oscillations within parietal and medial-temporal regions during spatial navigation. We speculate that the theta and gamma oscillations are coherent, providing a mechanism by which medial-temporal and parietal brain regions communicate during navigation—an important piece of the puzzle currently missing from the spatial navigation literature (Moser et al., 2008). Interestingly, it has been suggested that findings from spatial navigation research may provide insights into other aspects of cognitive brain function (Buzsáki, 2005), and mounting evidence suggests a functional link between theta and gamma oscillatory activity and cortico-hippocampal communication as part of a broader mechanism of processing within the brain (Babiloni et al., 2009; Lisman & Buzsáki, 2008; Sirota et al., 2008).

Hippocampal Activity, Theta Rhythm, and Scalp EEG

Although medial-temporal activity reported herein included activity in medial-temporal voxels, there exists a view that the hippocampus is a closed field structure and, thus, does not contribute to scalp-recorded EEG. Owing to its cylindrical structure, it has been proposed that neurons of the hippocampus form a radially symmetric field, and there is evidence to suggest some aspects of hippocampal activity are not detected immediately beyond the structure itself (Rosburg et al., 2007; Fernández, Klaver, Fell, Grunwald, & Elger, 2002; Fernández et al., 1999). However, early modeling on which this notion was based employed a simplified closed sphere of simultaneously active neurons not designed to simulate the hippocampus (Klee & Rall, 1977) and more recent modeling of deep brain structures, including the hippocampus, challenge the notion that hippocampal activity cannot be detected using EEG and MEG recordings (Attal et al., 2009). Given these unresolved issues, combined with the use of a standard head model, we take the conservative view that the medial-temporal lobe activity reported herein reflects parahippocampal theta activity. Given the strength of afferent and efferent hippocampal projections with the surrounding parahippocampal regions (indeed, parahippocampal cortex "accounts for the large majority of the cortical input to the hippocampus," Burwell, 2000, p. 25), such activity may provide an ideal window on hippocampal function using noninvasive recordings. Future research incorporating task-related iEEG from hippocampal regions and surface EEG recordings will enable greater insights as to the contribution of hippocampal activity in surface recorded EEG.

Source Localization with AJDC and sLORETA

EEG recordings from a given electrode sensor represent the summed activity of multiple source signals, plus extracerebral sources (e.g., EOG), as a result of volume conduction (see Congedo et al., 2008, for a review). When exploring deeper cortical sources, these effects are exacerbated, making source localization attempts from EEG even more difficult (e.g., Wagner et al., 2004). BSS methods such as AJDC may be a suitable method for counteracting volume conduction effects which lead to the "poor spatial resolution" of EEG recordings. Although source localization of ERP data has provided suggestive evidence of memory-related medial-temporal lobe activity, averaged responses across many trials are required to enhance signal-to-noise ratio (Alhaj, Massey, & McAllister-Williams, 2006). BSS techniques combined with source localization provide a useful tool for exploring task-related EEG (e.g., Delorme, Westerfield, et al., 2007) as well as applications in real-time EEG fields such as neurofeedback and brain–computer interfaces (Congedo, 2006) and clinical studies comparing patients to normative databases (Congedo et al., 2010).

Limitations and Conclusions

The use of a resting eyes-open "baseline" condition for comparison is a common method adopted in a variety of fields in cognitive neuroscience but is not without problems (e.g., Stark & Squire, 2001). Pretask resting conditions have been shown to have their own electrophysiological correlates (Chen, Feng, Zhao, Yin, & Wang, 2008; González-Hernández et al., 2005), suggesting caution is necessary when interpreting analyses with a resting eyes open comparison condition. Although a line-following control condition has been used in fMRI and PET navigation studies (e.g., Iaria et al., 2007; Hartley et al., 2003), EEG studies have reported theta and gamma activity associated with a number of behaviors associated with virtual movement (Jacobs et al., 2010; Caplan et al., 2003), suggesting a line-following control is inappropriate in such studies. de Araújo et al. (2002) explored an appropriate control condition in a MEG study of human navigation, focussing on theta activity. These researchers excluded frontal midline theta, the motor demands of the task, and passive viewing of the visual environment as factors explaining enhanced theta in virtual town navigation, albeit using MEG sensors largely distributed over temporal regions. Finally, after reporting, no differences between eyes-open resting and stationary route-planning conditions, navigation data were compared with a pooled control condition using both of these stationary conditions. Scalp maps of theta activity associated with navigation in the present study also indicated that

increased theta activity originated from posterior scalp sites and not frontal midline locations. Although the present findings require replication and extension, viewed in light of the correlation between the observed theta activity and navigation performance, the use of an eyes-open resting condition for comparison appears sufficient.

A further limitation of our study is the use of a standard head model and standard electrode coordinates, which lowers the spatial resolution and precision of our analysis. A better procedure would be to use individual head models and actual electrode coordinates to compute the inverse solution in each individual and then coregister the result in a standard head model.

Brain oscillatory activity associated with human spatial navigation has been difficult to study because of the depth of implicated brain regions and the limited information gained from traditional analysis of noninvasive recording techniques. Using AJDC coupled with source localization, two source components were found to show navigation-related activity: a right parietal source largely with gamma activation and a right medial-temporal–parietal source with theta and gamma activation. These findings further suggest theta activity is involved in integrating information from medial-temporal and parietal regions active during spatial processing while also implicating gamma activity in this role. Developing analysis techniques, such as AJDC coupled with source localization procedures, may enable insights into deeper brain processes from surface EEG recordings.

Acknowledgments

The authors thank the assistance of Julian Brown with task development and image preparation, Shaun Seixas with EEG data collection, and the anonymous reviewers for their valuable comments.

Reprint requests should be sent to David J. White, Brain and Psychological Sciences Research Centre, Brain Sciences Institute, Swinburne University of Technology, 427–451 Burwood Road, Hawthorn, Victoria, Australia 3122, or via e-mail: dawhite@groupwise.swin.edu.au, david_white_1@hotmail.com.

Notes

1. Available for free download at www.lis.inpg.fr/pages_perso/congedo/MC_Software.html.
2. At a less stringent level of significance ($p < .05$), a number of other sources displayed spectral power differences from baseline to navigation. These included a posterior alpha source (maximal in precuneus) demonstrating significantly greater 9–13 Hz activity during baseline than navigation. Furthermore, a source localized to the left precentral regions showed greater relative power from 9 to 12 Hz during baseline and significantly elevated 43–44 Hz absolute power during navigation. This likely reflected motor processing associated with right-hand keyboard presses required for navigation.
3. A complete reanalysis of the data with a broader frequency range was carried out to provide a confirmatory analysis of gamma findings. To facilitate analysis with a sampling rate of 128, data were band-pass filtered in the range 1–64 Hz. Artifact reduction and group BSS were applied as described. Very similar sources, both in terms of spatial localization and spectral properties, were observed as part of the BSS results. Most pertinent, Component 5 showed a similar source profile, with three of the strongest nine voxels localized to parahippocampal gyrus and three in the precuneus. Contrasting spectral power on this source during navigation with baseline showed significantly ($p < .05$) increased 3–5 Hz activity as well as 44–47, 52–53, and 55–63 Hz activity. These results confirmed the observation of increased gamma activity on the medial temporal/parietal source.

REFERENCES

Alhaj, H. A., Massey, A. E., & McAllister-Williams, R. H. (2006). Effects of DHEA administration on episodic memory, cortisol and mood in healthy young men: A double-blind, placebo-controlled study. *Psychopharmacology, 188,* 541–551.

Astur, R. S., Taylor, L. B., Mamelak, A. N., Philpott, L., & Sutherland, R. J. (2002). Humans with hippocampus damage display severe spatial memory impairments in a virtual Morris water maze. *Behavioral Brain Research, 132,* 77–84.

Attal, Y., Bhattacharjee, M., Yelnik, J., Cottereau, B., Lefèvre, J., Okada, J., et al. (2009). Modelling and detecting deep brain activity with MEG and EEG. *Ingénierie et Recherche Biomédicale, 30,* 133–138.

Babiloni, C., Vecchio, F., Mirabella, G., Buttiglione, M., Sebastiano, F., Picardi, A., et al. (2009). Hippocampal, amygdala, and neocortical synchronization of theta rhythms is related to an immediate recall during Rey Auditory Verbal Learning Test. *Human Brain Mapping, 30,* 2077–2089.

Bastiaansen, M., & Hagoort, P. (2003). Event-induced theta responses as a window on the dynamics of memory. *Cortex, 39,* 967–992.

Bischof, W. F., & Boulanger, P. (2003). Spatial navigation in virtual reality environments: An EEG analysis. *Cyberpsychology & Behavior, 6,* 487–495.

Bloomfield, P. (2000). *Fourier analysis of time series* (2nd ed.). New York: John Wiley & Sons.

Bohbot, V. D., Kalina, M., Stepankova, K., Spackova, N., Petrides, M., & Nadel, L. (1998). Spatial memory deficits in patients with lesions to the right hippocampus and to the right parahippocampal cortex. *Neuropsychologia, 36,* 1217–1238.

Burgess, N. (2008). Spatial cognition and the brain. *Annals of the New York Academy of Sciences, 1124,* 77–97.

Burwell, R. D. (2000). The parahippocampal region: Corticocortical connectivity. *Annals of the New York Academy of Sciences, 911,* 25–42.

Buzsáki, G. (2005). Theta rhythm of navigation: Link between path integration and landmark navigation, episodic and semantic memory. *Hippocampus, 15,* 827–840.

Byrne, P., Becker, S., & Burgess, N. (2007). Remembering the past and imagining the future: A neural model of spatial memory and imagery. *Psychological Review, 114,* 340–375.

Caplan, J. B., Madsen, J. R., Raghavachari, S., & Kahana, M. J. (2001). Distinct patterns of brain oscillations underlie to basic parameters of human maze learning. *Journal of Neurophysiology, 86,* 368–380.

Caplan, J. B., Madsen, J. R., Schulze-Bonhage, A., Aschenbrenner-Scheibe, R., Newman, E. L., & Kahana, M. J. (2003). Human theta oscillations related to sensorimotor integration and spatial learning. *Journal of Neuroscience, 23,* 4726–4736.

Chen, A. C. N., Feng, W., Zhao, H., Yin, Y., & Wang, P. (2008). EEG default mode network in the human brain: Spectral regional field powers. *Neuroimage, 41,* 561–574.
Collins, D. L., Neelin, P., Peters, T. M., & Evans, A. C. (1994). Automatic 3D intersubject registration of MR volumetric data in standardized Talairach space. *Journal of Computer Assisted Tomography, 18,* 192–205.
Congedo, M. (2006). Subspace projection filters for real-time brain electromagnetic imaging. *IEEE Transactions on Bio-Medical Engineering, 53,* 1624–1634.
Congedo, M., Gouy-Pailler, C., & Jutten, C. (2008). On the blind source separation of human electroencephalogram by approximate joint diagonalization of second order statistics. *Clinical Neurophysiology, 119,* 2677–2686.
Congedo, M., John, E. R., De Ridder, D., & Prichep, L. (2010). Group independent component analysis of resting-state EEG in large normative samples. *International Journal of Psychophysiology, 78,* 89–99.
Congedo, M., Ozen, C., & Sherlin, L. (2002). Notes on EEG resampling by natural cubic spline interpolation. *Journal of Neurotherapy, 6,* 73–80.
Cornwell, B. R., Johnson, L. L., Holroyd, T., Carver, F. W., & Grillon, C. (2008). Human hippocampal and parahippocampal theta during goal-directed spatial navigation predicts performance on a virtual Morris water maze. *Journal of Neuroscience, 28,* 5983–5990.
Cornwell, B. R., Salvadore, G., Colon-Rosario, V., Latov, D. R., Holroyd, T., Carver, F. W., et al. (2010). Abnormal hippocampal functioning and impaired spatial navigation in depressed individuals: Evidence from whole-head magnetoencephalography. *American Journal of Psychiatry, 167,* 836–844.
de Araújo, D. B., Baffa, O., & Wakai, R. T. (2002). Theta oscillations and human navigation: A magnetoencephalography study. *Journal of Cognitive Neuroscience, 14,* 70–78.
Delorme, A., Sejnowski, T., & Makeig, S. (2007). Enhanced detection of artifacts in EEG data using higher-order statistics and independent component analysis. *Neuroimage, 34,* 1443–1449.
Delorme, A., Westerfield, M., & Makeig, S. (2007). Medial prefrontal theta bursts precede rapid motor responses during visual selective attention. *Journal of Neuroscience, 27,* 11949–11959.
Ekstrom, A. D., Caplan, J. B., Ho, E., Shattuck, K., Fried, I., & Kahana, M. J. (2005). Human hippocampal theta activity during virtual navigation. *Hippocampus, 15,* 881–889.
Ekstrom, A. D., Kahana, M. J., Caplan, J. B., Fields, T. A., Isham, E. A., Newman, E. L., et al. (2003). Cellular networks underlying human spatial navigation. *Nature, 25,* 184–187.
Fernández, G., Effern, A., Grunwald, T., Pezer, N., Lehnertz, K., Dümpelmann, M., et al. (1999). Real-time tracking of memory formation in the human rhinal cortex and hippocampus. *Science, 285,* 1582–1585.
Fernández, G., Klaver, P., Fell, J., Grunwald, T., & Elger, C. E. (2002). Human declarative memory function: Separating rhinal and hippocampal contributions. *Hippocampus, 12,* 514–519.
Fiori, S. (2003). Overview of independent component analysis technique with an application to synthetic aperture radar (SAR) imagery processing. *Neural Network, 16,* 453–467.
González-Hernández, J. A., Céspedes-Garcia, Y., Campbell, K., Scherbaum, W. A., Bosch-Bayard, J., & Figueredo-Rodríguez, P. (2005). A pre-task resting condition neither "baseline" nor "zero." *Neuroscience Letters, 391,* 43–47.
Grau, C., Fuentemilla, L., & Marco-Pallarés, J. (2007). Functional neural dynamics underlying auditory event-related N1 and N1 suppression response. *Neuroimage, 36,* 522–531.
Grön, G., Wunderlich, A. P., Spitzer, M., Tomczak, R., & Riepe, M. W. (2000). Brain activation during human navigation: Gender-different neural networks as substrate of performance. *Nature Neuroscience, 3,* 404–408.
Hafting, T., Fyhn, M., Molden, S., Moser, M.-B., & Moser, E. I. (2005). Microstructure of a spatial map in the entorhinal cortex. *Nature, 436,* 801–806.
Hartley, J., Maguire, E. A., Spiers, H. J., & Burgess, N. (2003). The well-worn route and the path less traveled: Distinct neural bases of route following and wayfinding in humans. *Neuron, 7,* 877–888.
Hori, E., Nishio, Y., Kazui, K., Umeno, K., Tabuchi, E., Sasaki, K., et al. (2005). Place-related neural responses in the monkey hippocampal formation in a virtual space. *Hippocampus, 15,* 991–996.
Huang, R. S., Jung, T. P., Delorme, A., & Makeig, S. (2008). Tonic and phasic electroencephalographic dynamics during continuous compensatory tracking. *Neuroimage, 39,* 1896–1909.
Iaria, G., Chen, J. K., Guariglia, C., Ptito, A., & Petrides, M. (2007). Retrosplenial and hippocampal brain regions in human navigation: Complimentary functional contributions to the formation and use of cognitive maps. *European Journal of Neuroscience, 25,* 890–899.
Jacobs, J., Korolev, I. O., Caplan, J. B., Ekstrom, A. D., Litt, B., Baltuch, G., et al. (2010). Right-lateralized brain oscillations in human spatial navigation. *Journal of Cognitive Neuroscience, 22,* 824–836.
James, C. J., & Hesse, C. W. (2005). Independent component analysis for biomedical signals. *Physiological Measurement, 26,* R15–R39.
Jang, G. J., Lee, T. W., & Oh, Y. H. (2002). Learning statistically efficient features for speaker recognition. *Neurocomputing, 49,* 329–348.
Kahana, M. J., Sekuler, R., Caplan, J. B., Kirschen, M., & Madsen, J. R. (1999). Human theta oscillations exhibit task dependence during virtual maze navigation. *Nature, 399,* 781–784.
Klee, M., & Rall, W. (1977). Computed potentials of cortically arranged populations of neurons. *Journal of Neurophysiology, 40,* 647–666.
Leal, A. J. R., Dias, A. I., Vieira, J. P., Moreira, A., Távora, L., & Calado, E. (2008). Analysis of the dynamics and origin of epileptic activity in patients with tuberous sclerosis evaluated for surgery of epilepsy. *Clinical Neurophysiology, 119,* 853–861.
Leal, A. J. R., Nunes, S., Dias, A. I., Vieira, J. P., Moreira, A., & Calado, E. (2007). Analysis of the generators of epileptic activity in early-onset childhood benign occipital lobe epilepsy. *Clinical Neurophysiology, 118,* 1341–1347.
Lee, A. C. H., Buckley, M. J., Pegman, S. J., Spiers, H., Scahill, V. L., Gaffan, D., et al. (2005). Specialization in the medial temporal lobe for processing of objects and scenes. *Hippocampus, 15,* 782–797.
Lisman, J. (2005). The theta/gamma discrete phase code occurring during the hippocampal phase precession may be a more general brain coding scheme. *Hippocampus, 15,* 913–922.
Lisman, J., & Buzsáki, G. (2008). A neural coding scheme formed by the combined function of gamma and theta oscillations. *Schizophrenia Bulletin, 34,* 974–980.
Lorente de Nò, R. (1947). Action potential of motoneurons of the hypoglossus nucleus. *Journal of Cellular and Comparative Physiology, 29,* 207–287.
Mackay, J. C., Kirk, I. J., Hamm, J. P., & Johnson, B. W. (2001). Human theta oscillations in virtual maze navigation and Sternberg tasks. *International Journal of Neuroscience, 109,* 180.

Maguire, E. A., Burgess, N., Donnett, J. G., Frackowiak, R. S. J., Frith, C. D., & O'Keefe, J. (1998). Knowing where and getting there: A human navigation network. *Science, 280,* 921–924.

Marco-Pallarés, J., Grau, C., & Ruffini, G. (2005). Combined ICA-LORETA analysis of mismatch negativity. *Neuroimage, 25,* 471–477.

Matsumura, N., Nishijo, H., Tamura, R., Eifuku, S., Endo, S., & Ono, T. (1999). Spatial- and task-dependent neuronal responses during real and virtual translocation in the monkey hippocampal formation. *Journal of Neuroscience, 19,* 2381–2393.

Moser, E. I., Kropff, E., & Moser, M. B. (2008). Place cells, grid cells, and the brain's spatial representation system. *Annual Review of Neuroscience, 31,* 69–89.

Mutihac, R., & Mutihac, R. C. (2007). A comparative study of independent component analysis algorithms for electroencephalography. *Romanian Reports in Physics, 59,* 831–860.

Nunez, P. L., & Srinivasan, R. (2006). *Electric fields of the brain: The neurophysics of EEG* (2nd ed.). New York: Oxford University Press.

Nunn, J. A., Graydon, F. J. X., Polkey, C. E., & Morris, R. G. (1999). Differential spatial memory impairment after right temporal lobectomy demonstrated using temporal titration. *Brain, 122,* 47–59.

O'Keefe, J., & Nadel, L. (1978). *The hippocampus as a cognitive map*. Oxford: Oxford University Press.

Onton, J., Delorme, A., & Makeig, S. (2005). Frontal midline EEG dynamics during working memory. *Neuroimage, 27,* 341–356.

Onton, J., Westerfield, M., Townsend, J., & Makeig, S. (2006). Imaging human EEG dynamics using independent component analysis. *Neuroscience & Biobehavioral Reviews, 30,* 808–822.

Parslow, D. M., Morris, R. G., Fleminger, S., Rahman, Q., Abrahams, S., & Recce, M. (2005). Allocentric spatial memory in humans with hippocampal lesions. *Acta Psychologica, 118,* 123–147.

Pascual-Marqui, R. D. (2002). Standardized low resolution brain electromagnetic tomography (sLORETA): Technical details. *Methods & Findings in Experimental & Clinical Pharmacology, 24(Suppl. D),* 5–12.

Romero, S., Mañanas, M. A., & Barbanoj, M. J. (2008). A comparative study of automatic techniques for ocular artifact reduction in spontaneous EEG signals based on clinical target variables: A simulation case. *Computers in Biology & Medicine, 38,* 348–360.

Rosburg, T., Trautner, P., Ludowig, E., Scaller, C., Kurthen, M., Elger, C. E., et al. (2007). Hippocampal event-related potentials to tone duration deviance in a passive oddball paradigm in humans. *Neuroimage, 37,* 274–281.

Seixas, S., Brotchie, P., Crewther, D., & Ip, S. (2006). Spatial coordinate systems within the parietal lobes: Localization of a cognitive spatial map in humans. *Clinical EEG & Neuroscience, 37,* 167–168.

Sirota, A., Montgomery, S., Fujisawa, S., Isomura, Y., Zugaro, M., & Buzsáki, G. (2008). Entrainment of neocortical neurons and gamma oscillations by the hippocampal theta rhythm. *Neuron, 60,* 683–697.

Stark, C. E. L., & Squire, L. R. (2001). When zero is not zero: The problem of ambiguous baseline conditions in fMRI. *Proceedings of the National Academy of Sciences, U.S.A., 98,* 12760–12766.

Talairach, J., & Tournoux, P. (1988). *Co-planar stereotaxic atlas of the human brain: Three-dimensional proportional system*. Stuttgart: Georg Thieme.

Tesche, C. D., & Karhu, J. (2000). Theta oscillations index human hippocampal activation during a working memory task. *Proceedings of the National Academy of Sciences, U.S.A., 97,* 919–924.

Tichavský, P., & Yeredor, A. (2009). Fast approximate joint diagonalization incorporating weight matrices. *IEEE Transactions on Signal Processing, 57,* 878–891.

Towle, V. L., Bolaños, J., Suarez, D., Tan, K., Grzeszczuk, R., Levin, D. N., et al. (1993). The spatial location of EEG electrodes: Locating the best fitting sphere relative to cortical anatomy. *Electroencephalography and Clinical Neuroscience, 86,* 1–6.

van der Loo, E., Congedo, M., Plazier, M., Van de Heyning, P., & De Ridder, D. (2007). Correlation between independent components of scalp EEG and intracranial EEG (iEEG) time series. *International Journal of Bioelectromagnetism, 9,* 270–275.

van der Veen, A. J., Talwar, S., & Paulraj, A. (1997). A subspace approach to blind space-time signal processing for wireless communication systems. *IEEE Transactions on Signal Processing, 45,* 173–190.

Wagner, M., Fuchs, M., & Kastner, J. (2004). Evaluation of sLORETA in the presence of noise and multiple sources. *Brain Topography, 16,* 277–280.

Welch, P. D. (1967). The use of Fast Fourier Transform for the estimation of power spectra: A method based on time averaging over short, modified periodograms. *IEEE Transactions on Audio & Electroacoustics, 15,* 70–74.

Westfall, P. H., & Young, S. S. (1993). *Resampling-based multiple testing*. New York: John Wiley & Sons.

Whitlock, J. R., Sutherland, R. J., Witter, M. P., Moser, M. B., & Moser, E. I. (2008). Navigating from hippocampus to parietal cortex. *Proceedings of the National Academy of Sciences, U.S.A., 105,* 14755–14762.

Yuen, P. C., & Lai, J. H. (2002). Face representation using independent component analysis. *Pattern Recognition, 35,* 1247–1257.